

Submitted to the
XXII International Symposium on Lepton-Photon Interactions at High
Energy
30 June - 5 July, Uppsala, Sweden

Abstract: 266

Session: QCD/HS, FP

Measurements of charm fragmentation ratios and fractions in deep inelastic scattering at HERA

ZEUS Collaboration

Abstract

Charm production in deep inelastic scattering has been measured with the ZEUS detector at HERA using an integrated luminosity of approximately 82 pb^{-1} . Charm has been tagged by reconstructing $D^{*\pm}$, D^0 , D^\pm , D_s^\pm and Λ_c^\pm charm hadrons in the kinematic region $1.5 < Q^2 < 1000 \text{ GeV}^2$, $0.02 < y < 0.7$, $p_T(D, \Lambda_c) > 3 \text{ GeV}$ and $|\eta(D, \Lambda_c)| < 1.6$. The charm fragmentation ratios and fractions are measured in the kinematic range considered.

1 Introduction

Charm quarks in photoproduction and deep inelastic scattering (DIS) have been extensively studied at HERA [1–6]. These measurements are consistent with perturbative QCD calculations indicating boson-gluon fusion (BGF) as the dominant mechanism of charm production. For most of the charm DIS measurements only D^* mesons are selected.

This paper presents the measurements of charm production in DIS using D^0 , D^\pm , D_s^\pm and $D^{*\pm}$ mesons and Λ_c^\pm baryons. Measurements of the charm fragmentation ratios and fractions were performed in ep scattering at HERA in the DIS regime with $1.5 < Q^2 < 1000 \text{ GeV}^2$. The results are compared with previous measurements in e^+e^- annihilations and also at HERA.

2 Experimental set-up

The data presented in this analysis were collected with the ZEUS detector at HERA during the 1998-2000 running periods, with e^\pm beam energy of $E_e = 27.5 \text{ GeV}$ colliding with a proton beam energy of $E_p = 920 \text{ GeV}$. The data sample corresponds to an integrated luminosity of 82 pb^{-1} .

A detailed description of the ZEUS detector can be found elsewhere [7]. A brief outline of the components that are most relevant for this analysis is given below.

Charged particles are tracked in the central tracking detector (CTD) [8], which operates in a magnetic field of 1.43 T provided by a thin superconducting solenoid. The CTD consists of 72 cylindrical drift chamber layers, organised in nine superlayers covering the polar-angle¹ region $15^\circ < \theta < 164^\circ$. The transverse-momentum resolution for full-length tracks is $\sigma(p_T)/p_T = 0.0058p_T \oplus 0.0065 \oplus 0.0014/p_T$, with p_T in GeV .

The high-resolution uranium–scintillator calorimeter (CAL) [9] consists of three parts: the forward, the barrel and the rear calorimeters. The smallest subdivision of the calorimeter is called a cell. The CAL energy resolutions, as measured under test-beam conditions, are $\sigma(E)/E = 0.18/\sqrt{E}$ for electrons and $\sigma(E)/E = 0.35/\sqrt{E}$ for hadrons, with E in GeV .

¹ The ZEUS coordinate system is a right-handed Cartesian system, with the Z axis pointing in the proton beam direction, referred to as the “forward direction”, and the X axis pointing left towards the centre of HERA. The coordinate origin is at the nominal interaction point.

3 Event selection

An event was selected if it satisfied the following criteria: a scattered electron was identified using a neural-network procedure [10] with energy $E'_e > 10$ GeV; $y_e \leq 0.95$; $y_{\text{JB}} \geq 0.02$; $1.5 < Q_\Sigma^2 < 1000$ GeV², where the subscripts e , JB and Σ refer to the electron, Jaquet-Blondel [11] and Σ - [12] methods, respectively; $40 < \delta < 65$ GeV, where $\delta = \sum_i (E - p_z)_i$ and the index i runs over a combination of tracks measured in CTD and CAL clusters; a reconstructed primary vertex with $|Z_{\text{vertex}}| < 50$ cm is required; the impact point (X, Y) for the scattered lepton in the RCAL must lie outside the region 26×14 cm² centred on $X = Y = 0$.

The selected kinematic region was $1.5 < Q^2 < 1000$ GeV² and $0.02 < y < 0.7$.

4 Reconstruction of charm hadrons

The reconstruction of D^0 , D^\pm , D_s^\pm , $D^{*\pm}$ mesons and Λ_c^\pm baryons was performed in the kinematic region $p_T(D, \Lambda_c) > 3.0$ GeV and $|\eta(D, \Lambda_c)| < 1.6$. The distributions were fitted assuming a “modified” Gaussian function, $\text{Gauss}^{\text{mod}} \propto \exp(-0.5x^{1+\frac{1}{1+0.5x}})$, where $x = |(M - M_{D, \Lambda_c})/\sigma|$, to describe the signal shape plus a background function. Only tracks measured in the CTD and fitted to the primary vertex were used in the reconstruction.

4.1 Reconstruction of D^0 mesons

The D^0 mesons were reconstructed from the decay channel $D^0 \rightarrow K^- \pi^+$ (+c.c.). In each event, D^0 candidates are formed from pairs of tracks with opposite charges and $p_T > 0.8$ GeV. A cut $|\cos \theta^*(K)| < 0.85$, where $\theta^*(K) = \text{angle}(\mathbf{p}_K^{(D^0 \text{ rest})}, \mathbf{p}_{D^0}^{(\text{lab})})$, was applied to reduce the contribution from combinatorial background. The D^0 candidates were separated in two groups. The “ ΔM tag” group consists of D^0 candidates which are combined with a third track that could be a “soft” pion (π_s) in a $D^{*+} \rightarrow D^0 \pi_s^+$ (+ c.c.) decay. The soft pion must have $p_T > 0.2$ GeV and charge opposite to that of the kaon. The cut value was $p_T > 0.25$ GeV for a data subsample, corresponding to an integrated luminosity of 17 pb^{-1} , for which the track reconstruction efficiency at low-momentum was smaller due to the operating conditions of the CTD [13]. For D^0 mesons not coming from a $D^{*\pm}$, the incorrect assignment of the pion and kaon masses to the two tracks produces a wider reflected signal. The reflected signal normalised to the ratio of numbers of D^0 without and with ΔM tag is subtracted from the untagged D^0 candidates. Figures 1 and 2 show the $M(K\pi)$ distribution for untagged D^0 candidates after the reflection subtraction and tagged D^0 candidates, respectively. Clear signals are seen at the

nominal value of $M(D^0)$. The number of D^0 untag (tag) mesons yielded by the fit was $N^{\text{untag}}(D^0) = 9910 \pm 940$ ($N^{\text{tag}}(D^0) = 1907 \pm 77$).

4.2 Reconstruction of additional $D^{*\pm}$ mesons

The $D^{*\pm}$ mesons were reconstructed from the decay channels $D^{*+} \rightarrow D^0\pi_s^+$ (+c.c.) with $D^0 \rightarrow K^-\pi^+$ (+c.c.). The $D^{*\pm}$ events within the $D^{*\pm}$ kinematic range can be considered as the sum of events with D^0 events within D^0 kinematic range (tagged D^0) plus D^0 events not in that kinematic range. In each event, pairs of tracks with $p_T > 0.4$ GeV were combined to form a D^0 candidate. Only combinations with invariant mass $1.80 < M(K\pi) < 1.92$ GeV were considered. Besides that, the D^0 candidates must have $p_T(D^0) < 3.0$ GeV or $|\eta(D^0)| > 1.6$ to be outside the kinematic region. A third track with $p_T > 0.2$ GeV and charge opposite to that of the kaon track was combined with the D^0 candidate to form a $D^{*\pm}$ candidate, and kept if its charge was opposite to the kaon track. Here again the cut value was $p_T > 0.25$ GeV for the data subsample for which the track reconstruction efficiency at low-momentum was smaller. Figure 3 shows the distribution of the mass difference $\Delta M = M(K\pi\pi_s) - M(K\pi)$ for D^* candidates. A clear signal is seen around the nominal value of $M(D^{*\pm}) - M(D^0)$. The combinatorial background under the signal was estimated from the mass difference distribution of the wrong-charge combinations, in which both tracks associated to the D^0 candidate have the same charge and the third track has opposite charge. The number of reconstructed additional $D^{*\pm}$ mesons was calculated by subtracting the wrong-charge ΔM distribution, after normalising it to the number of right-charge candidates in the region $0.150 < \Delta M < 0.165$ GeV. The subtraction was done in the signal region $0.143 < \Delta M < 0.148$ GeV and yielded $N^{\text{add}}(D^{*\pm}) = 312 \pm 28$.

4.3 Reconstruction of D^\pm mesons

The D^\pm mesons were reconstructed from the decay channel $D^\pm \rightarrow K^-\pi^+\pi^+$ (+c.c.). In each event, two tracks with the same charges and a third track with opposite charge were combined to form D^\pm candidates. Tracks were required to have $p_T(\pi) > 0.5$ GeV and $p_T(K) > 0.7$ GeV. To reduce the combinatorial background, a cut in the variable $\cos\theta^*(K) > -0.75$ is imposed, where $\theta^*(K) = \text{angle}(\mathbf{p}_K^{(D^\pm \text{ rest})}, \mathbf{p}_{D^\pm}^{\text{(lab)}})$. To suppress background from $D^{*\pm}$ and D_s^\pm no combination with $M(K\pi\pi) - M(K\pi) < 0.150$ GeV and with $M(K^\pm \text{“}K^\mp\text{”})$ within ± 8 MeV of the nominal ϕ mass was taken [3]. Figure 4 shows the $M(K\pi\pi)$ distributions for D^\pm candidates. A clear signal is seen at the nominal value of $M(D^\pm)$. The number of D^\pm mesons yielded by the fit was $N(D^\pm) = 3530 \pm 360$.

4.4 Reconstruction of D_s^\pm mesons

The D_s^\pm mesons were reconstructed from the decay channel $D_s^+ \rightarrow \phi\pi^+$ (+c.c.) with $\phi \rightarrow K^+K^-$. In each event, two tracks with opposite charges were combined to form the ϕ candidates whose invariant mass $M(KK)$ should be within ± 8 MeV of the nominal ϕ mass [3]. A third track was combined with the ϕ candidate yielding the D_s^\pm candidate. Only tracks with $p_T(\pi) > 0.5$ GeV and $p_T(K) > 0.7$ GeV were considered. Combinatorial background was suppressed with the following cuts: $|\cos^3 \theta^{**}(K)| > 0.1$ and $\cos \theta^*(\pi) < 0.85$, where $\theta^{**}(K) = \text{angle}(\mathbf{p}_K^{(\phi \text{ rest})}, \mathbf{p}_\pi^{(\phi \text{ rest})})$ and $\theta^*(\pi) = \text{angle}(\mathbf{p}_\pi^{(D_s \text{ rest})}, \mathbf{p}_{D_s}^{(\text{lab})})$. Figure 5 shows the $M(KK\pi)$ distribution for D_s candidates. A clear signal is seen at the nominal value of $M(D_s^\pm)$. A secondary signal also appears at the nominal value of $M(D^\pm)$, as expected from the decay of D^\pm in the same channel. The resulting mass distribution was fitted to the sum of two modified Gaussians, one for each signal peak. The number of reconstructed D_s^\pm mesons yielded by the fit was $N(D_s^\pm) = 680 \pm 79$.

4.5 Reconstruction of Λ_c^\pm baryons

The Λ_c^\pm baryons were reconstructed from the decay channel $\Lambda_c^+ \rightarrow K^-p\pi^+$ (+c.c.). In each event, two tracks with the same charges and a third track with opposite charge were combined to form the Λ_c^\pm candidates. Only tracks with $p_T(\pi) > 0.5$ GeV, $p_T(K) > 0.75$ GeV and $p_T(p) > 1.3$ GeV were considered. The proton momentum in the laboratory frame is typically larger than that of the pion from the decay due to the large difference of their masses. Therefore, of the two tracks with same charges, to the one with larger (smaller) momentum was assigned the proton (pion) mass. The mass of the kaon was assigned to the track with opposite charge. To suppress the combinatorial background the following cuts were applied: $\cos \theta^*(K) > -0.9$ and $\cos \theta^*(p) > -0.25$, where $\theta^*(K, p) = \text{angle}(\mathbf{p}_{K,p}^{(\Lambda_c \text{ rest})}, \mathbf{p}_{\Lambda_c}^{(\text{lab})})$. Figure 6 shows the $M(pK\pi)$ distribution for Λ_c candidates. The number of reconstructed Λ_c baryons yielded by the fit was $N(\Lambda_c^\pm) = 630 \pm 250$.

5 Charm fragmentation ratios and fractions ²

5.1 Ratio of neutral and charged D mesons production rates

The ratio of neutral and charged D meson production rates, $R_{u/d}$, is the ratio of the sum of direct neutral mesons (D^{*0} , D^0) production cross sections to the sum of the charged

² For all charm fragmentation ratios and fractions the distortions from decays of excited D mesons with non-zero orbital momentum were neglected.

mesons ($D^{*\pm}$, D^\pm) production cross sections. Direct production of D^0 and D^\pm means these mesons do not originate from D^{*0} and $D^{*\pm}$ decays. As all D^{*0} 's decay into D^0 , the ratio is given by

$$R_{u/d} = \frac{\sigma^{\text{untag}}(D^0)}{\sigma(D^\pm) + \sigma^{\text{tag}}(D^0)}.$$

The ratio of neutral and charged D meson production rates obtained for the kinematic region $1.5 < Q^2 < 1000 \text{ GeV}^2$, $0.02 < y < 0.7$, $p_T(D, \Lambda_c) > 3.0 \text{ GeV}$ and $|\eta(D, \Lambda_c)| < 1.6$ is

$$R_{u/d} = 1.46 \pm 0.17^{+0.10}_{-0.34}.$$

The measured ratio is consistent with one. The large systematic effect comes mainly from the signal extraction procedure which also affects the other measurements of ratios and fractions.

The measurement is compared with other values obtained at HERA [14,15] and with those from e^+e^- annihilations [16–18] in Figure 7. All measurements agree within experimental uncertainties.

5.2 Strangeness suppression factor

The strangeness suppression factor γ_s is the ratio of twice the cross sections for charmed meson containing a strange quark divided by the cross sections for those containing an up or down quark. As all D^{*+} and D^{*0} decay into either a D^+ or a D^0 and all D_s^{*+} decay into a D_s^+ , γ_s is the ratio of twice the D_s^+ cross section to the sum of the equivalent D^0 and D^+ cross sections. Equivalent cross sections were defined as the the sums of D^0 and D^+ direct cross sections and contributions from D^{*+} and D^{*0} decays. The strangeness suppression factor is then given by

$$\gamma_s = \frac{2\sigma(D_s^\pm)}{\sigma(D^\pm) + \sigma^{\text{untag}}(D^0) + \sigma^{\text{tag}}(D^0) + 2\sigma^{\text{add}}(D^{*\pm})}.$$

The strangeness suppression factor obtained for the kinematic region $1.5 < Q^2 < 1000 \text{ GeV}^2$, $0.02 < y < 0.7$, $p_T(D, \Lambda_c) > 3.0 \text{ GeV}$ and $|\eta(D, \Lambda_c)| < 1.6$ is

$$\gamma_s = 0.265 \pm 0.035^{+0.039}_{-0.048}.$$

The measurement is compared with other values obtained at HERA [14,15,19] and with those from e^+e^- annihilations [20] in Figure 7. All measurements agree within experimental uncertainties.

5.3 Fraction of D mesons produced in a vector state

The fraction of D mesons produced in a vector state is given by the ratio of vector charm-meson production cross sections to the sum of vector and direct pseudoscalar charm-meson production cross sections. The fraction for charged charm-mesons is given by

$$P_V^d = \frac{\sigma^{\text{tag}}(D^0)/B_{D^{*+} \rightarrow D^0 \pi^+} + \sigma^{\text{add}}(D^{*\pm})}{\sigma(D^\pm) + \sigma^{\text{tag}}(D^0) + \sigma^{\text{add}}(D^{*\pm})},$$

where $B_{D^{*+} \rightarrow D^0 \pi^+} = 0.677 \pm 0.005$ [21] is the branching ratio of the $D^{*+} \rightarrow D^0 \pi^+$ decay.

The fraction of D mesons produced in a vector state for the charged and neutral charm-mesons, considering the same production rates for D^{*0} and $D^{*\pm}$, is given by

$$P_V = \frac{2\sigma^{\text{tag}}(D^0)/B_{D^{*+} \rightarrow D^0 \pi^+} + 2\sigma^{\text{add}}(D^{*\pm})}{\sigma(D^\pm) + \sigma^{\text{untag}}(D^0) + \sigma^{\text{tag}}(D^0) + 2\sigma^{\text{add}}(D^{*\pm})}.$$

The fractions P_V^d and P_V measured for the kinematic region $1.5 < Q^2 < 1000$ GeV², $0.02 < y < 0.7$, $p_T(D, \Lambda_c) > 3.0$ GeV and $|\eta(D, \Lambda_c)| < 1.6$ are, respectively,

$$P_V^d = 0.590 \pm 0.037_{-0.018}^{+0.022},$$

$$P_V = 0.490 \pm 0.032_{-0.019}^{+0.071}.$$

It can be seen from the measured fractions P_V^d and P_V that naive spin counting, which predicts a value of 0.75, does not hold for charm production.

The measurements are compared with other values obtained at HERA [14, 15] and with those from e^+e^- annihilations [16–18] in Figure 7. All measurements agree within experimental uncertainties.

5.4 Charm fragmentation fractions

The fraction of c quarks hadronising into a particular charm hadron, $f(c \rightarrow D, \Lambda_c)$, is the ratio of the charmed-hadron production rate to the sum of the production rate of all charm ground states. The strange-charm baryons Ξ_c^\pm , Ξ_c^0 and Ω_c^0 cross sections should be included in the sum in addition to the measured D mesons and Λ_c baryons. The production rates for these baryons is expected to be much lower than that for Λ_c^\pm due to strangeness suppression. The relative rates for these baryons can be estimated from the non-charm sector as in [22]. Assuming equal production of Ξ^\pm and Ξ^0 and that the measured non-charmed Ξ^-/Λ and Ω^-/Λ relative rates, $(6.65 \pm 0.28)\%$ and $(0.42 \pm 0.07)\%$, respectively [21], are similar to the charmed ones, the total rate for the charm-strange baryons should be about $(14 \pm 5)\%$ of the Λ_c production rate. Also considering the same

production rates for D^{*0} and $D^{*\pm}$, the sum of the production rates for all charm ground states is

$$\sum_{all} \sigma_{g.s.} = \sigma(D^\pm) + \sigma^{\text{untag}}(D^0) + \sigma^{\text{tag}}(D^0) + 2\sigma^{\text{add}}(D^{*\pm}) + \sigma(D_s^\pm) + \sigma(\Lambda_c^\pm) \times 1.14.$$

Therefore, the charm fragmentation fractions are:

$$f(c \rightarrow D^0) = [\sigma^{\text{untag}}(D^0) + \sigma^{\text{tag}}(D^0) + \sigma^{\text{add}}(D^{*\pm}) \times (1 + B_{D^{*+} \rightarrow D^0 \pi^+})] / \sum_{all} \sigma_{g.s.},$$

$$f(c \rightarrow D^{*+}) = [\sigma^{\text{tag}}(D^0) / B_{D^{*+} \rightarrow D^0 \pi^+} + \sigma^{\text{add}}(D^{*+})] / \sum_{all} \sigma_{g.s.},$$

$$f(c \rightarrow D^+) = [\sigma(D^+) + \sigma^{\text{add}}(D^{*+}) \times (1 - B_{D^{*+} \rightarrow D^0 \pi^+})] / \sum_{all} \sigma_{g.s.},$$

$$f(c \rightarrow D_s^+) = \sigma(D_s^+) / \sum_{all} \sigma_{g.s.},$$

$$f(c \rightarrow \Lambda_c^+) = \sigma(\Lambda_c^+) / \sum_{all} \sigma_{g.s.},$$

The measured fragmentation fractions are shown in Table 1.

The measurements are compared with other values obtained at HERA [14, 15, 19] and with those from e^+e^- annihilations [20] in Figure 8. All measurements agree within experimental uncertainties.

6 Summary

The production of D^0 , D^\pm , D_s^\pm and $D^{*\pm}$ charm mesons and Λ_c^\pm charm baryons has been measured in DIS at HERA in the kinematic region $1.5 < Q^2 < 1000 \text{ GeV}^2$, $0.02 < y < 0.7$, $p_T(D, \Lambda_c^\pm) > 3.0 \text{ GeV}$ and $|\eta(D, \Lambda_c^\pm)| < 1.6$ with the ZEUS detector. The ratio of neutral and charged D -meson production rates, the strange suppression factor, the fraction of charged and the sum of charged and neutral charm mesons produced in a vector state and the fractions of c quarks hadronising as D^0 , D^\pm , D_s^\pm , $D^{*\pm}$ and Λ_c^\pm hadrons were determined in the above kinematic range. All fragmentation ratios and fractions agree with those obtained in charm production at HERA and in e^+e^- annihilations, confirming the universality of charm fragmentation.

References

- [1] ZEUS Coll., S. Chekanov et al., Phys. Rev. **D 69**, 0120004 (2004).
- [2] H1 Coll., C. Adloff et al., Phys. Lett. **B 528**, 199 (2002).
- [3] ZEUS Coll., J. Breitweg et al., Phys. Lett. **B 481**, 213 (2000).
- [4] ZEUS Coll., J. Breitweg et al., Eur. Phys. J. **C 12**, 35 (2000).
- [5] H1 Coll., C. Adloff et al., Nucl. Phys. **B 545**, 21 (1999).
- [6] ZEUS Coll., J. Breitweg et al., Eur. Phys. J. **C 6**, 67 (1999).
- [7] ZEUS Coll., U. Holm (ed.), *The ZEUS Detector*. Status Report (unpublished), DESY (1993), available on <http://www-zeus.desy.de/bluebook/bluebook.html>.
- [8] N. Harnew et al., Nucl. Inst. Meth. **A 279**, 290 (1989);
B. Foster et al., Nucl. Phys. Proc. Suppl. **B 32**, 181 (1993);
B. Foster et al., Nucl. Inst. Meth. **A 338**, 254 (1994).
- [9] M. Derrick et al., Nucl. Inst. Meth. **A 309**, 77 (1991);
A. Andresen et al., Nucl. Inst. Meth. **A 309**, 101 (1991);
A. Caldwell et al., Nucl. Inst. Meth. **A 321**, 356 (1992);
A. Bernstein et al., Nucl. Inst. Meth. **A 336**, 23 (1993).
- [10] H. Abramowicz, A. Caldwell and R. Sinkus, Nucl. Inst. Meth. **A 365**, 508 (1995).
- [11] F. Jacquet and A. Blondel, *Proceedings of the Study for an ep Facility for Europe*, U. Amaldi (ed.), p. 391. Hamburg, Germany (1979). Also in preprint DESY 79/48.
- [12] U. Bassler and G. Bernardi, Nucl. Inst. Meth. **A 361**, 197 (1995).
- [13] D. Bailey and R. Hall-Wilton, Nucl. Instrum. Meth. **A515**, 37 (2003).
- [14] ZEUS Coll., *Measurement of charm fragmentation ratios and fractions in γp collisions at HERA*, Abstract 564, International Europhysics Conference on High Energy Physics. Aachen, Germany (2003).
- [15] H1 Coll., A. Aktas et al., Eur. Phys. J. **C38**, 447 (2005).
- [16] DELPHI Coll., P. Abreu et al., Eur. Phys. J. **C12**, 225 (2000).
- [17] ALEPH Coll., R. Barate et al., Eur. Phys. J. **C16**, 597 (2000).
- [18] OPAL Coll., K. Ackerstaff et al., Eur. Phys. J. **C5**, 1 (1998).
- [19] ZEUS Coll., J. Breitweg et al., Phys. Lett. **B481**, 213 (2000).
- [20] L. Gladilin, Preprint hep-ex/9912064, 1999 (1999).
- [21] Particle Data Group, S. Eidelman et al., Phys. Lett. **B592**, 1 (2004).
- [22] OPAL Coll., G. Alexander et al., Z. Phys. **C72**, 1 (1996).

	ZEUS prel. (DIS)
$f(c \rightarrow D^0)$	$0.584 \pm 0.039_{-0.050}^{+0.024}$
$f(c \rightarrow D^{*\pm})$	$0.190 \pm 0.014_{-0.009}^{+0.023}$
$f(c \rightarrow D^\pm)$	$0.194 \pm 0.020_{-0.011}^{+0.023}$
$f(c \rightarrow D_s^\pm)$	$0.103 \pm 0.013_{-0.017}^{+0.012}$
$f(c \rightarrow \Lambda_c^\pm)$	$0.104 \pm 0.048_{-0.010}^{+0.018}$

Table 1: *The fractions of c quarks hadronising as a particular charm hadron.*

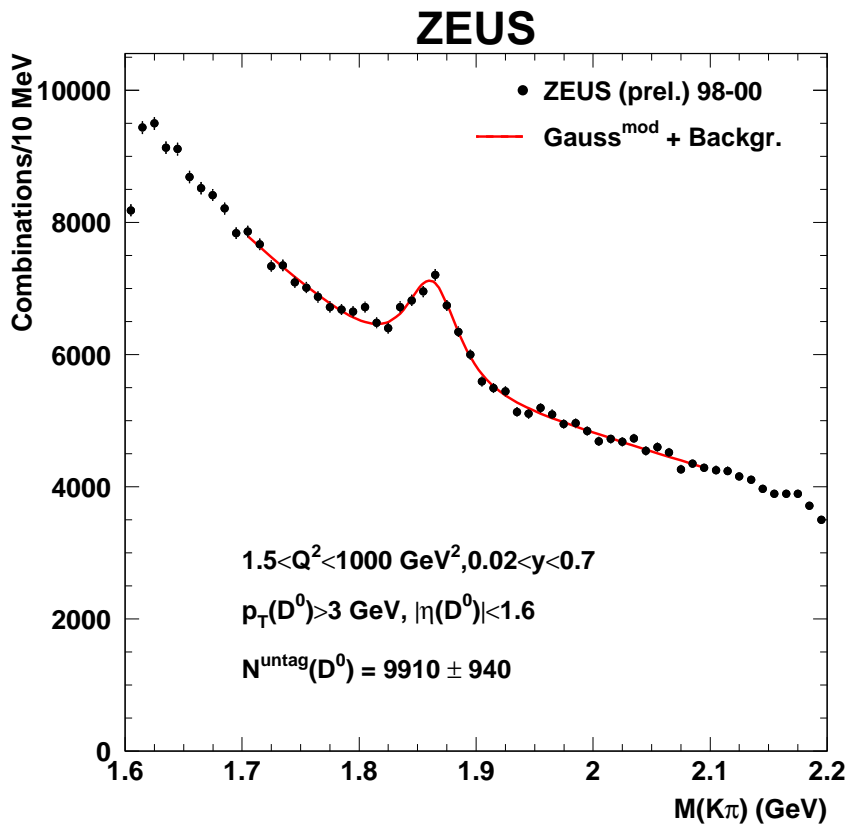


Figure 1: The $M(K\pi)$ distribution for the untagged D^0 candidates. The solid curve represents a fit to the sum of a modified Gaussian function and a background function.

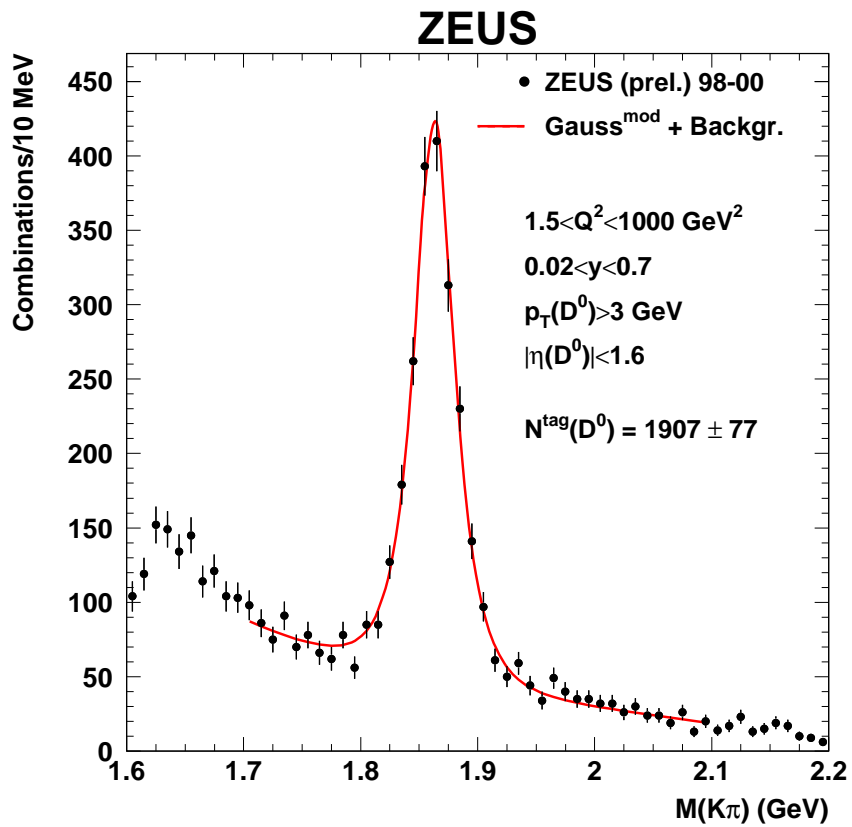


Figure 2: The $M(K\pi)$ distribution for the tagged D^0 candidates. The solid curve represents a fit to the sum of a modified Gaussian function and a background function.

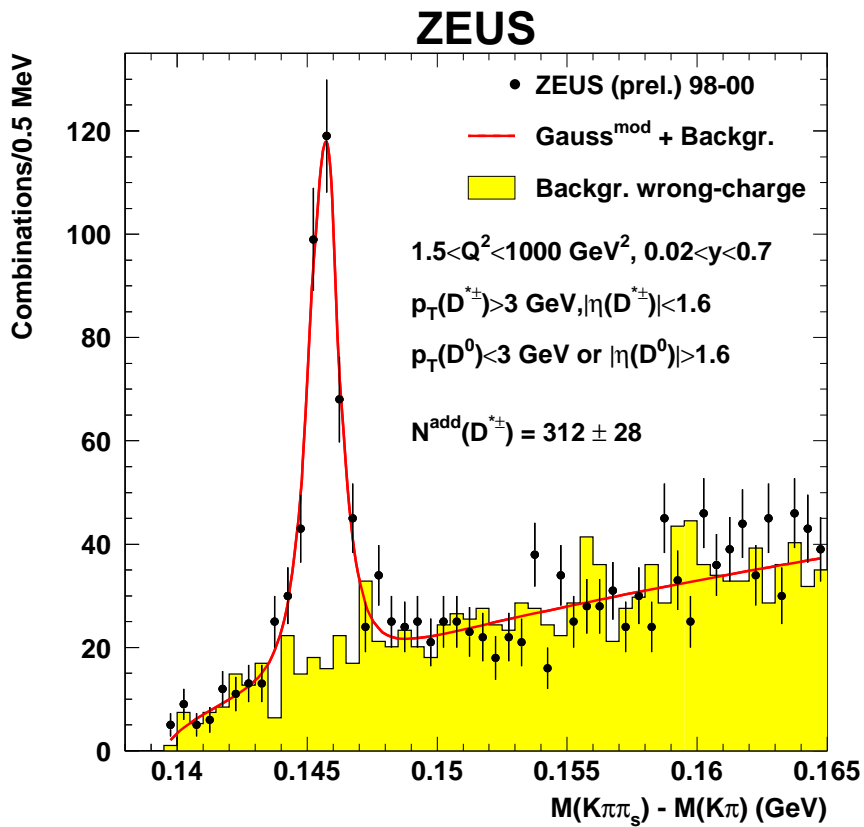


Figure 3: The distribution of the mass difference $\Delta M = M(K\pi\pi_s) - M(K\pi)$ for additional $D^{*\pm}$ candidates. The histogram shows the ΔM distribution for wrong-charge combinations. The solid curve represents a fit to the sum of a modified Gaussian function and a background function.

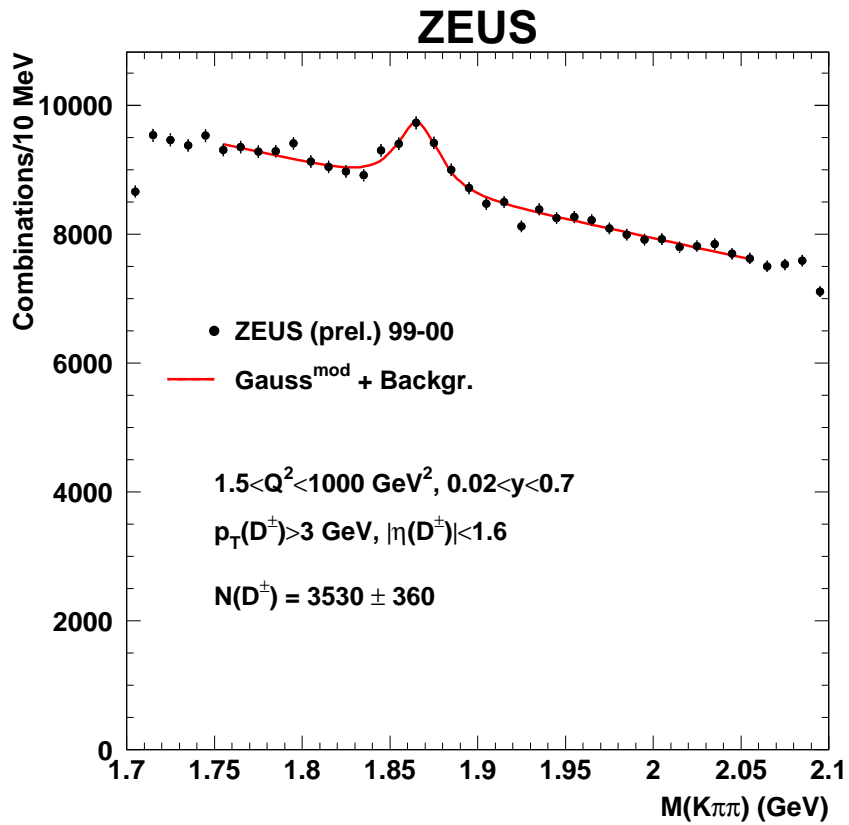


Figure 4: *The $M(K\pi\pi)$ distribution for the D^\pm candidates. The solid curve represents a fit to the sum of a modified Gaussian function and a background function.*

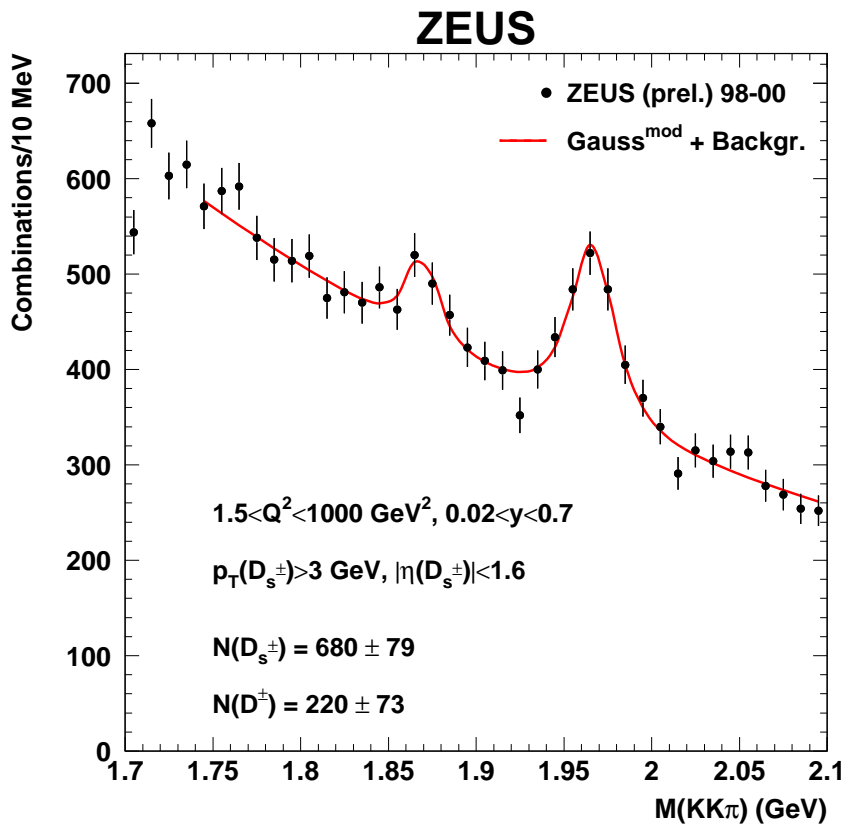


Figure 5: *The $M(KK\pi)$ distribution for the D_s candidates. The solid curve represents a fit to the sum of two modified Gaussian functions and a background function.*

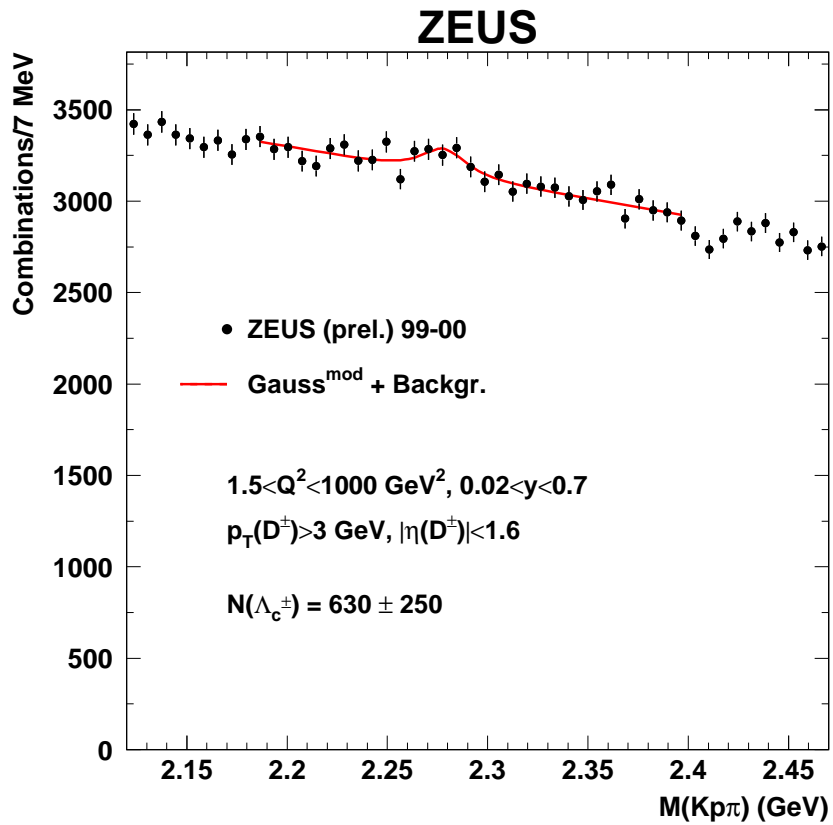


Figure 6: *The $M(pK\pi)$ distribution for the Λ_c candidates. The solid curve represents a fit to the sum of a modified Gaussian function and a background function.*

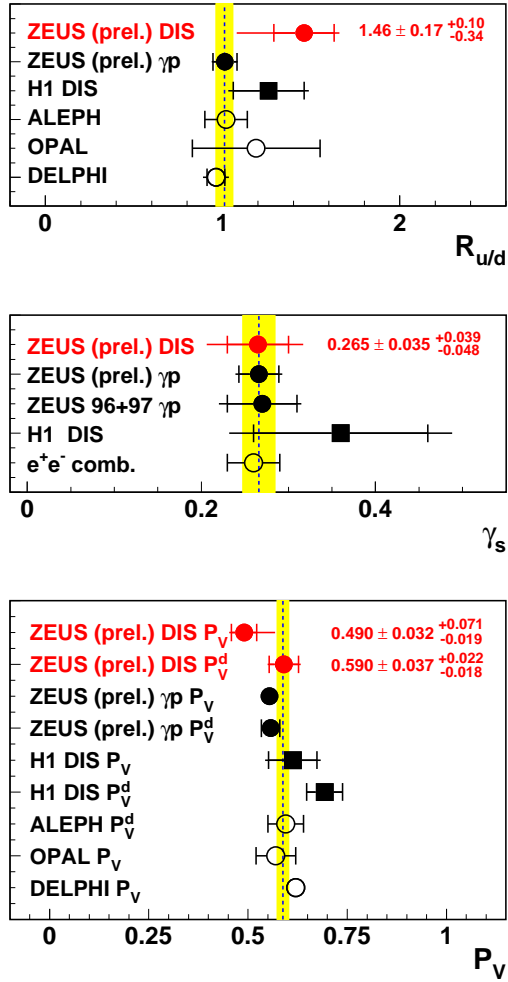


Figure 7: Comparison of the charm ratios measurements with those obtained in other experiments.

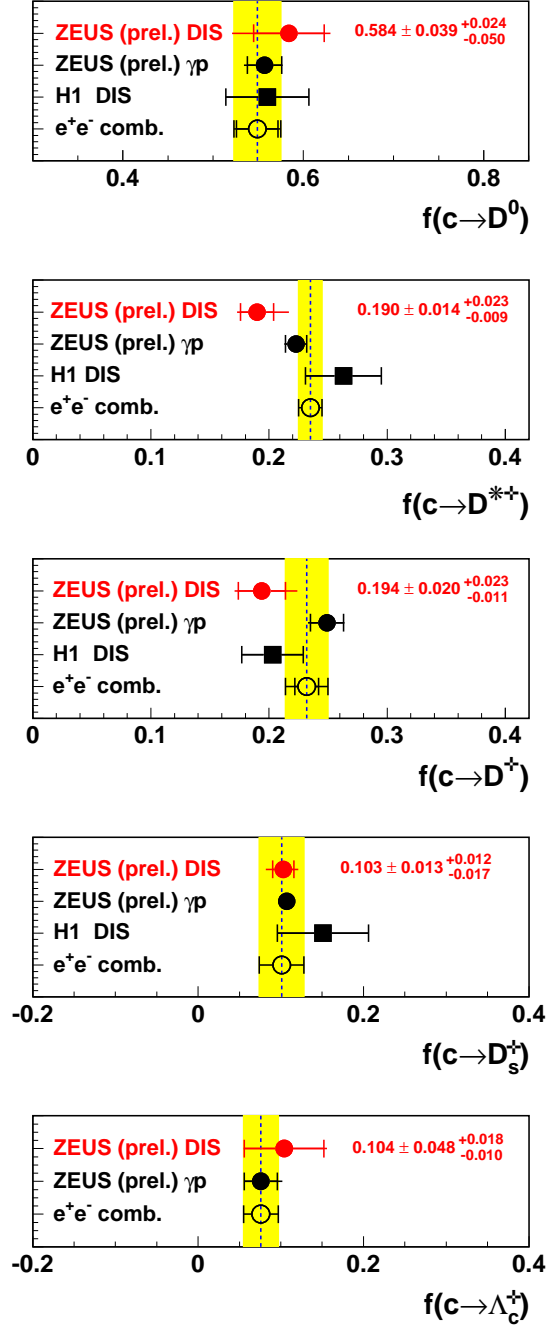


Figure 8: Comparison of the charm fragmentation fractions measurements with those obtained in other experiments.